Fundamental Studies on Electron Beam Welding of Heat-resistant Superalloys for Nuclear Plants (Report 4)†

— Temperature and Stress Distribution during Welding —

Yoshiaki ARATA*, Kiyohide TERAI, Hiroyoshi NAGAI***, Shigeki SHIMIZU***, Toshiichi AOTA*** and Yoshikazu IKEMOTO*****

Abstract

In this paper, temperature and stress distribution of the welds during welding was analyzed by means of finite element method, employing electron beam weld model and conventional one. Obtained conclusions can be summarized as follows:

1) In the nailhead neck area of the electron beam weld model, the peak temperature to be heated is higher than in other ones, and this area is exposed for longer time to the temperature above 1000°C than in other ones. Furthermore, tensile stress acts here both within wide range and above 1000°C. For this reason, microcrack is apt to occur in the nailhead neck area of the electron beam welds.

2) In the heat affected zone of the conventional weld model, the peak temperature to be heated is not so high as in that of electron beam weld model. Furthermore, the internal restraint intensity on cooling in the heat affected zone is smaller than that of the electron beam weld model. For this reason, microcrack does not occur in the conventional welds so often as in the electron beam welds.

1. Introduction

In the previous report[1], it was made clear that microcrack in the electron beam welds of heat-resistant superalloys for nuclear plants did occur almost perpendicularly to the fusion line. This microcrack was supposed to have initiated at the melted precipitate in the heat affected zone adjacent to the fusion line[2]. It is necessary, however, to explain the microcracking mechanism in further details that temperature and stress distribution during welding is fully clarified. Meanwhile, microcrack hardly occurred in the actual TIG welds.

In this paper, weld model similar to the actual electron beam welding was estimated and temperature and stress distribution of the heat affected zone during welding was analyzed by means of finite element method. Meanwhile, numerical solution was also conducted for the conventional weld model to make clear the difference due to welding process. Thereby, some useful results were obtained through this study to clarify the microcracking mechanism from viewpoint of temperature, stress and strain during welding.

2. Analytical Method

Numerical solution was carried out by means of finite element method. Non-steady state heat flow analysis and elastic plastic stress analysis were respectively performed by Wilson and Clough's method[3] and Yamada's method[4].

Table 1 shows the material constants of Inconel 617 at 1000°C which was proved in previous report[1] to be most susceptible to microcracking. In the analysis, temperature dependance of material constants was not taken into consideration. Moreover, work hardening of material was herein disregarded. Material was regarded as elastic and perfectly plastic body.

Table 1 Material Constants at 1000°C of Inconel 617

Young's Modulus (E)	1.372×10^5 (MPa)
Poisson's Ratio (ν)	0.307
Yield Stress (σ_Y)	78.4 (MPa)
Mean Expansion Coefficient (α)	1.625×10^{-5}
Density (ρ)	8.01 (g/cm^3)
Specific Heat (C)	0.158 (cal/g.°C)
Thermal Conductivity (k)	0.0683 (cal/cm. sec.°C)

† Received on April 17, 1978

* Professor, Director

** Visiting Professor of Ocean Engineering Department of MIT, USA

*** Kawasaki Heavy Industries, Ltd.

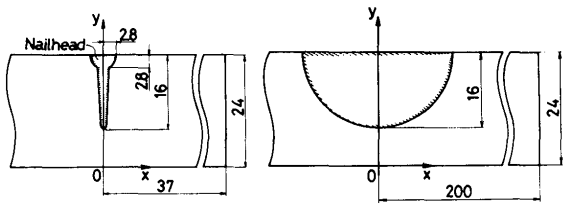

Fig. 1 Weld Model for Analysis (Unit: mm)
(a) Electron Beam Weld Model
(b) Conventional Weld Model

Fig. 1 shows the geometry of weld models for analysis and orthoganal coordinate system used in the numerical solution. The geometry of electron beam weld model was obtained by measuring the actual welds. Meanwhile, conventional welds geometry is assumed a little extremely to be semi-circular and of the same penetration depth as electron beam welds in order to make clear the appreciable difference of stress field resultant from welds geometry. This weld model is below mentioned as conventional weld model. The coordinate system is usually used with the plane of specimen's surface as X-Y plane. In this case, however, special interest is attracted on the distribution of both temperature and stress in the transverse cross-section during welding. Therefore, the coordinate system is employed with this transverse plane of the welds as X-Y plane.

Weld metal was herein assumed to be solid in the numerical solution even if it was above the melting temperature.

It was assumed as the initial conditions at the time of t=o(s) in the heat flow analysis that weld metal zone melted uniformly to be at 2000 °C and that other one was kept constant at 0 °C. It was also supposed as the boundary conditions that both edges of specimen in the X axis were kept constant at 0 °C and that heat loss from the surface of the specimen and latent heat in melting and solidification were respectively disregarded. Meanwhile, it was assumed as the initial conditions at the time of t=o(s) in the stress analysis that no stress acted in whole areas. In this case, no external restraint was augmented to the specimen because it was the purpose of this study to analyze the stress distribution due to the internal restraint. The analysis was carried out under the condition of σ_z=0, that was, in the plane stress condition.

Fig. 2 shows the finite element idealization. The elements adjacent to the fusion line are of nearly same size and placed almost within 0.3 to 0.4 mm in the perpendicular direction to fusion line. Triangular element which would accompany the linear variation of temperature and displacement in itself and quadrangular one which consists of triangular ones were respectively used for electron beam weld model and conventional one.

3. Analytical Results and Discussion

3.1 Characteristics of Distribution of Temperature and Stress in Electron Beam Weld Model

Fig. 3 describes the temperature distribution (isothermal contour) in the electron beam welds with the elapse of time. This isothermal contour was analyzed by the GPCP (General Purpose Contouring Program) of CALCOMP, based on the joint temperature obtained through the heat flow analysis. **Fig. 4** shows the temperature change at several typical points in

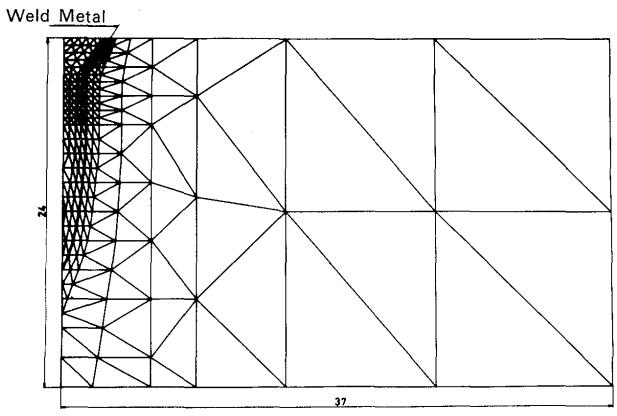

(a) Electron Beam Weld Model

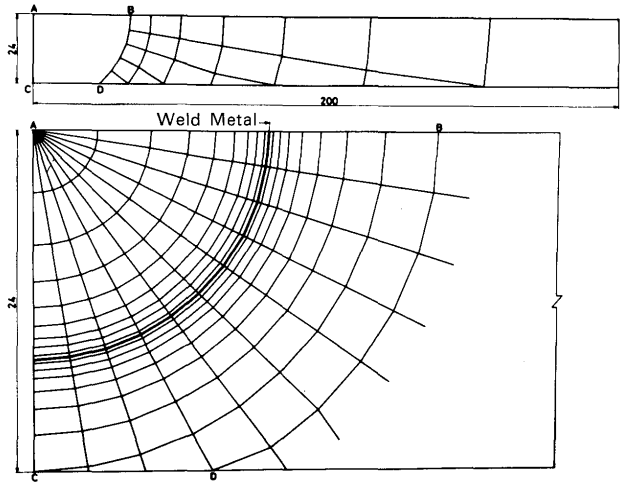

(b) Conventional Weld Model

Fig. 2 Finite Element Idealization of Model

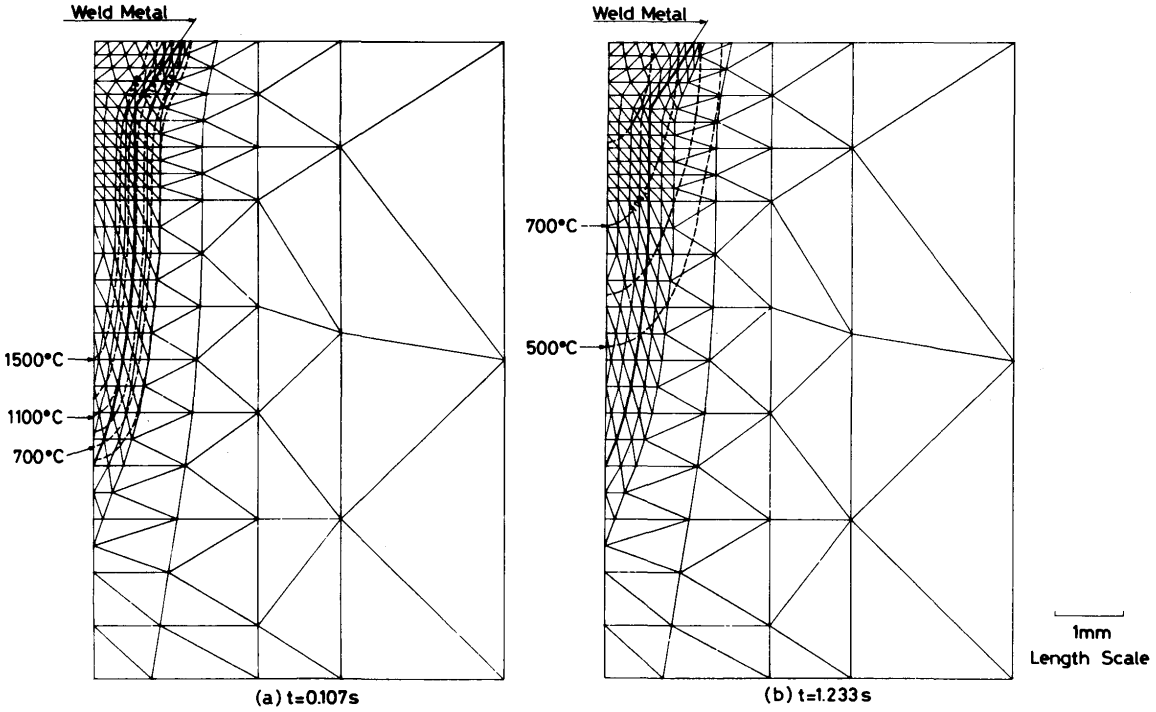

Fig. 3 Isothermal Contour during Electron Beam Welding

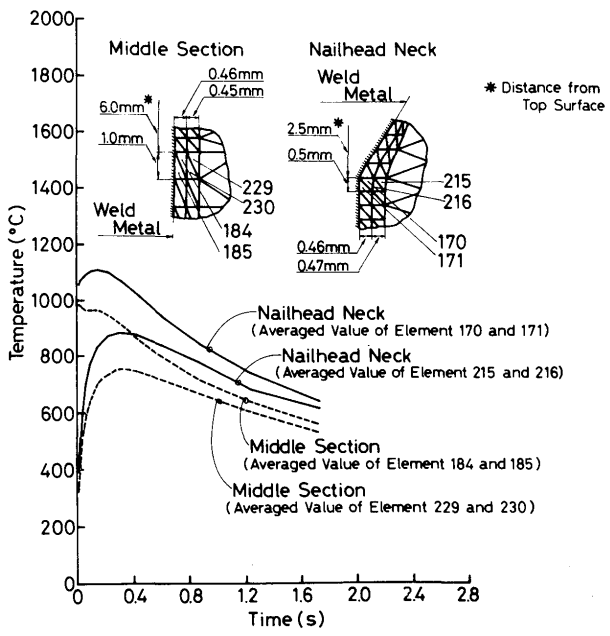

Fig. 4 Temperature Change in Heat Affected Zone Adjacent to Fusion Line (Electron Beam Weld Model)

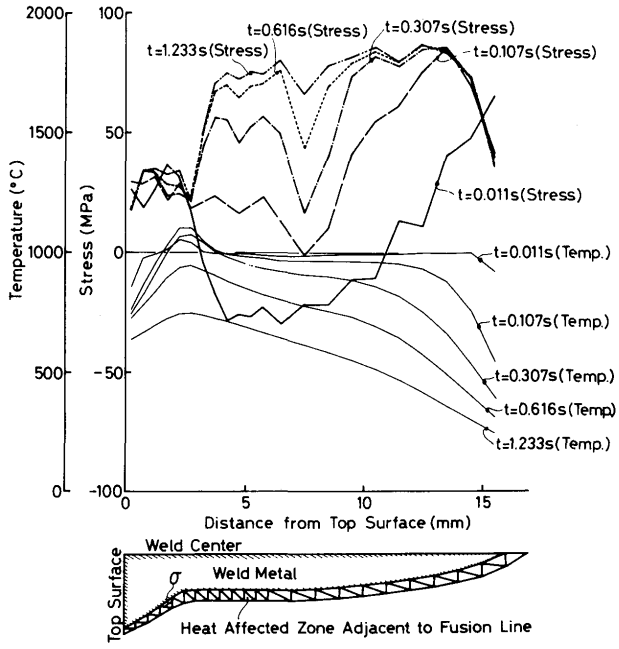

Fig. 5 Temperature and Stress Distribution in Heat Affected Zone Adjacent to Fusion Line (Electron Beam Weld Model)

the heat affected zone adjacent to the fusion line. **Fig. 5** shows the continuous distribution of temperature and parallel stress component to the fusion line in the heat affected zone adjacent to it. In Figs. 4 and 5, the temperature and stress are respectively weighted mean of the area between two adjacent triangular elements to the fusion line and plotted at the centroid of the compounded quadrangular element. From these figures, it may be safely the most noticeable characteristics of temperature distribution in the electron beam welds that the maximum

peak temperature to be heated occurs obviously in the nailhead neck area and this area is heated to the temperature above 1000 °C for longer time than other ones. This area is essentially apt to be heated within wide range to higher temperature than other ones. As mentioned above, such characteristics of the temperature distribution in the nailhead neck area are resultant from the local geometry of electron beam welds which may be regarded as one of some characteristics of weld bead by electron beam welding.

Meanwhile, as far as it concerns with the distribution of the parallel stress component to the fusion line, the middle section of the penetration depth receives the compressive stress still at the time of $t=0.011$(s). At both surface area and bottom section of the penetration depth, however, tensile stress acts even at that time. This is because the cooling rate is rather large at these areas. Both tensile stress zone and tensile plastic one spread further on and after that time in the heat affected zone. The amount of tensile stress in the nailhead neck area, however, doesn't increase so much. As a result, the stress amount in this area becomes considerably smaller than that in the deeper areas. It might be one of the main reasons that the compressive stress resultant from the local geometry acts perpendicularly to the fusion line. This stress may be a little overestimated because the molten metal is herein assumed to be solid. However, above-mentioned philosophy is considered to be reasonable because the solidifying molten metal certainly exists adjacently to the fusion line.

Fig. 6 shows the distribution of principal stress in the nailhead neck area with the elapse of time. As described in this figure, tensile stress acts in the heat affected zone near the fusion line and compressive one apart from this zone. The principal stress in the heat affected zone almost coincide with both the fusion line and isothermal contour in its direction. From the fact that the microcrack (hot crack) in the nailhead neck area did occur almost perpendicularly to the fusion line, this microcrack is supposed to have initiated at the melted precipitate and propagated due to this principal stress. The appreciable difference isn't seen between in the nailhead neck area and in other ones at the early stage. As the time goes on, the tensile stress obviously acts within rather wide range in the nailhead neck area than in other ones.

The main reason of microcrack in the nailhead neck area is generalized from the temperature and stress distribution during electron beam welding mentioned above as follows. In the nailhead neck area, the tensile stress amount is relatively somewhat small, but this stress acts along the fusion line above 1000 °C for longer time due to both higher peak temperature to be heated and longer time to be exposed above 1000 °C. Moreover, tensile stress acts here within rather wide range above 1000 °C because it decreases more gradually in this area than in other ones. Microcrack is supposed to have also occurred occasionally in the middle section of the actual electron beam welds because tensile stress amount is rather large here as shown in Fig. 5.

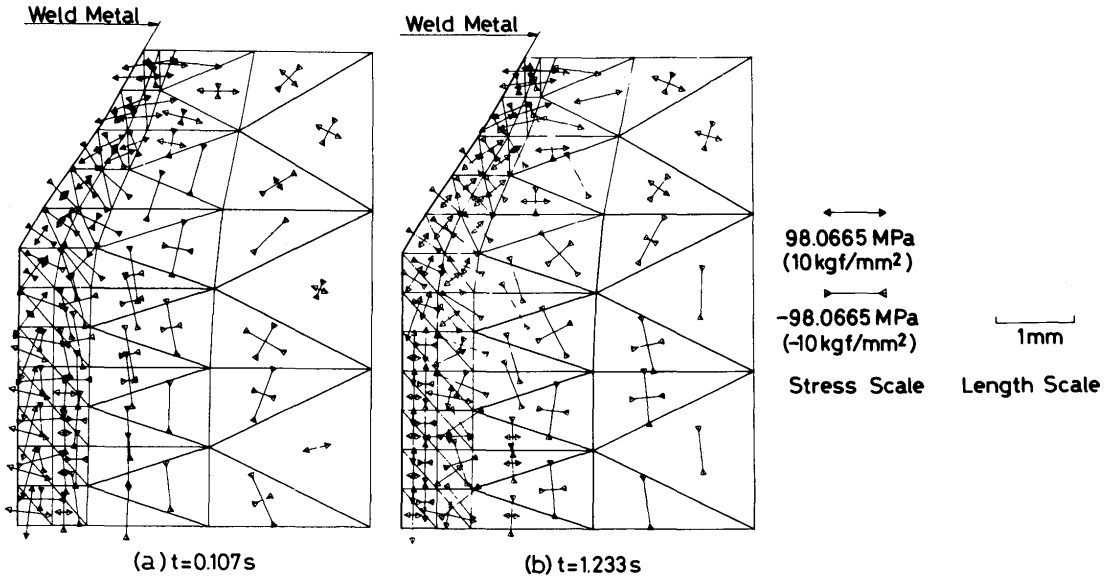

Fig. 6 Principal Stress Distribution during Electron Beam Welding

3.2 Comparison of Characteristic Distribution of Temperature and Stress between Electron Beam Weld Model and Conventional One

Fig. 7 shows the isothermal contour of the conventional weld model with the elapse of time. **Fig. 8** describes the temperature change at several typical points adjacent to the fusion line. **Fig. 9** shows the continuous distribution of temperature and parallel stress component to the fusion line. In Fig. 7, the isothermal contour was obtained also by the GPCP as in Fig. 3. From the temperature distribution of the conventional weld model, the peak temperature of the heat affected zone to be heated is below 1000 °C and lower by 100 °C approximately than in the electron beam weld model. Moreover, the heating rate and cooling one are extremely small. This can be supposed to be because the heat affected zone of conventional weld model is semicircular and quite different from the nailhead-like one of the electron beam weld model. From the distribution of stress component parallel to the fusion line, it is easily recognized that tensile stress zone is limited to the heat affected zone of surface area even at the cooling stage of 900 °C approximately and that conventional weld model essentially accompanies the low internal restraint intensity.

Fig. 10 shows the distribution of principal stress adjacent to the fusion line in the conventional weld model. It is recognized from this figure that the principal stress adjacent to the fusion line coincides in its direction with the fusion line and isothermal contour.

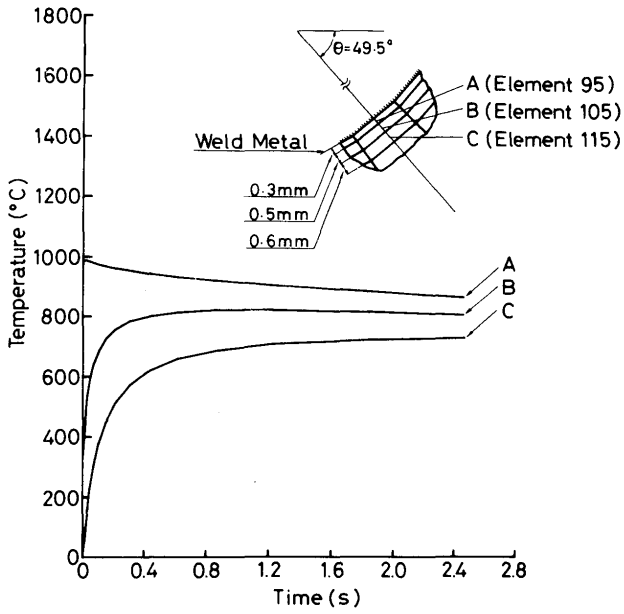

Fig. 8 Temperature Change in Heat Affected Zone Adjacent to Fusion Line (Conventional Weld Model)

Figs. 11 and **12** describe the stress and strain behavior at several typical points of the heat affected zone adjacent to the fusion line in electron beam weld model and conventional one respectively. The internal restraint intensity on cooling obtained from these figures is closely related to the susceptibility to hot cracking. Meanwhile, ${}_BT_R$ obtained in the hot ductility test is one of the important criteria to evaluate the susceptibility to microcracking. ${}_BT_R$ of

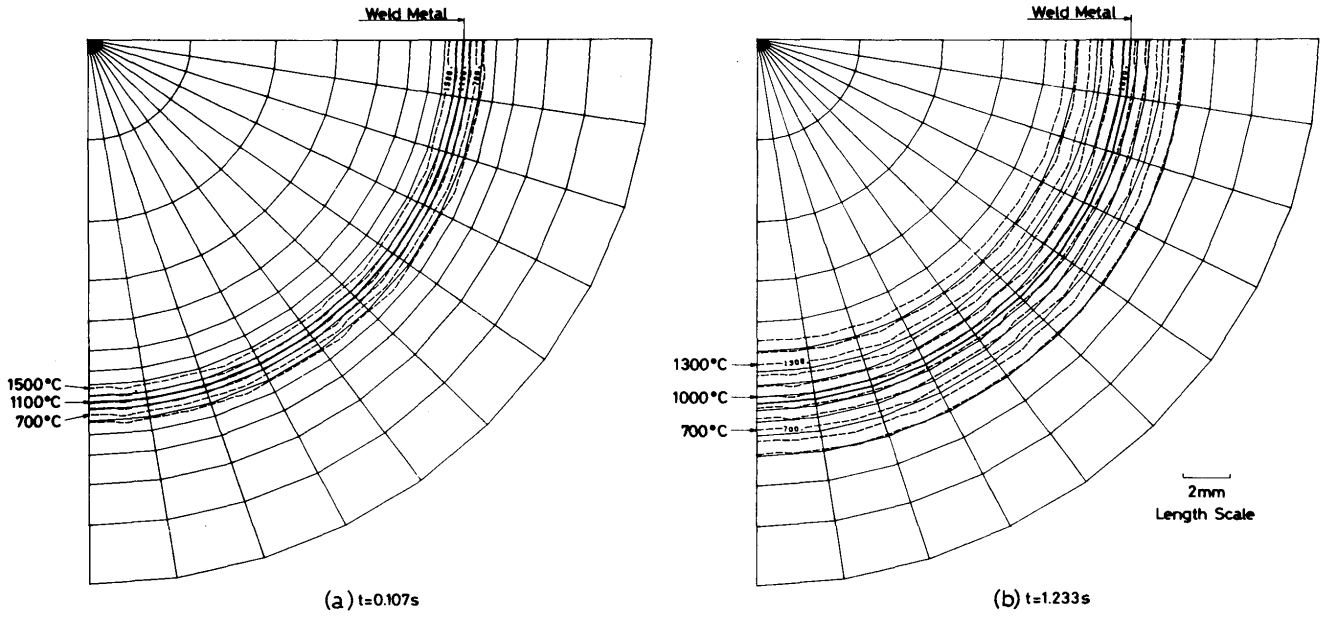

Fig. 7 Isothermal Contour during Conventional Welding

Inconel 617 is proved to be 265°C[5]. Therefore, the internal restraint intensity is below discussed on cooling from peak temperature to lower one by 250°C approximately than it. From the stress and strain behavior shown in Fig. 11, the nailhead neck area of electron beam weld model receives considerable compressive plastic deformation of 1.33% on heating from 0 to 976°C, and free expansion ($=1.62\times10^{-5}\times976=1.58\%$) is restrained by 80% approximately in its degree. On the other hand, free shrinkage is also restrained by 90% approximately on cooling from 1103 to 852°C. Meanwhile, it is the same case with the middle section of penetration depth. That is, free expansion on heating from 0 to 989°C and free shrinkage on cooling from 986 to 728°C are almost restrained. Therefore, it may be safely said that the heat affected zone of electron beam weld model receives high internal restraint. From the stress and strain behavior of the conventional weld mode shown in Fig. 12, it is clear at the bottom section of the penetration depth ($\theta=-85.5°$) that free expansion on heating from 0 to 980°C is almost restrained and free shrinkage on cooling from 908 to 736°C by 30% approximately. At the middle section of the penetration depth ($\theta=-49.5°$), free expansion on heating from 0 to 980°C is almost restrained and free shrinkage on cooling from 908°C to 747°C by 10% approximately. At the surface area ($\theta=-4.5°$), likewise, the free expansion on heating from 0 to 980°C is almost restrained and the free shrinkage on cooling from 980 to 724°C by 60% approximately. From the above-mentioned results, the heat affected zone of the conventional weld model receives compressive plastic deformation of the same degree as the electron beam welds on heating. On cooling, however, the internal restraint intensity is about one half or less than that of the electron beam weld model. This might be due to the smaller cooling rate and temperature gradient on cooling resultant from larger thermal capacity than electron beam weld model.

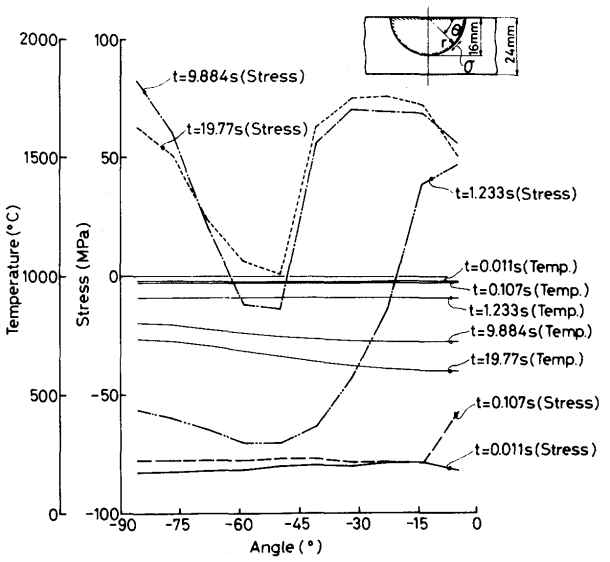

Fig. 9 Temperature and Stress Distribution in Heat Affected Zone Adjacent to Fusion Line (Conventional Weld Model)

It is supposed from the characteristics of stress and strain behavior mentioned above that microcrack tends to occur in the electron beam welds and that it hardly occurs in the conventional welds.

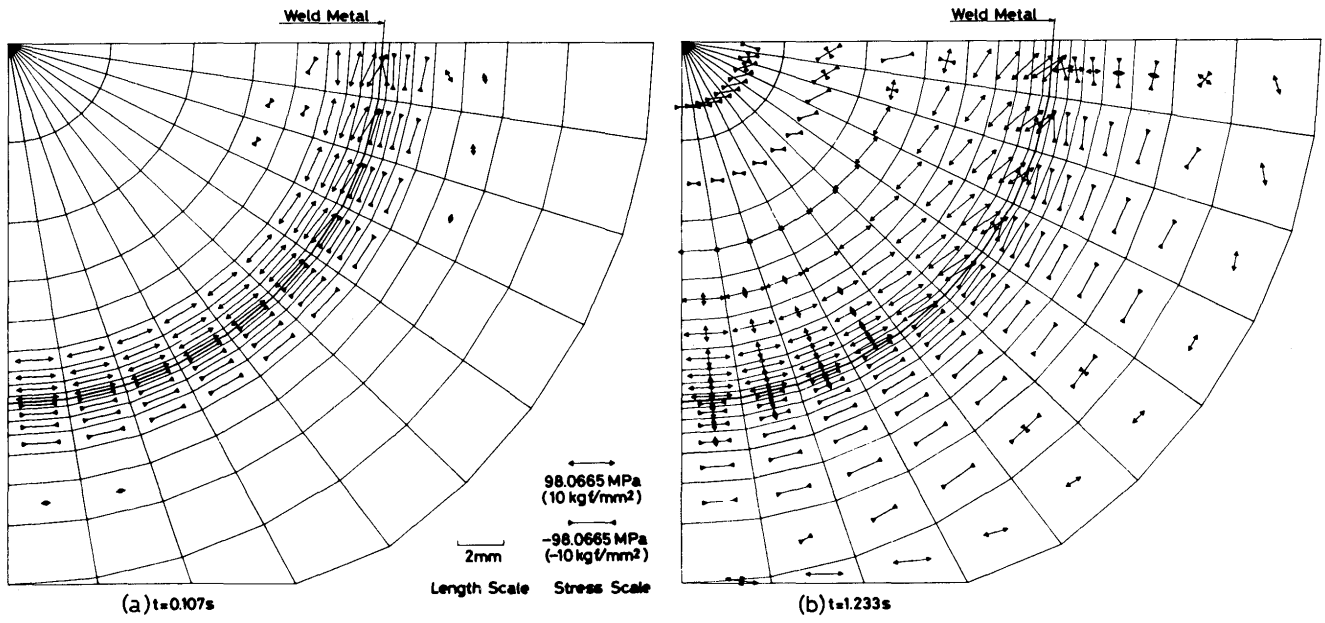

Fig. 10 Principal Stress Distribution during Conventional Welding

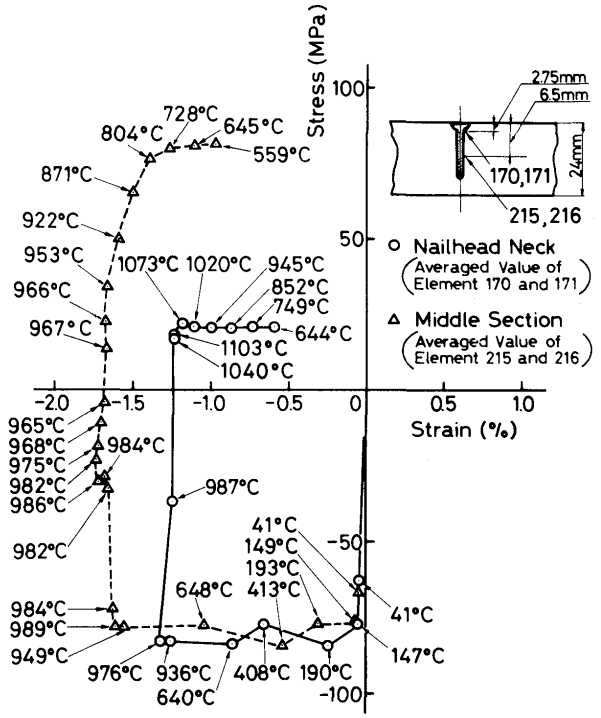

Fig. 11 Stress and Strain behavior in heat affected zone adjacent to fusion line (Electron Beam Weld Model)

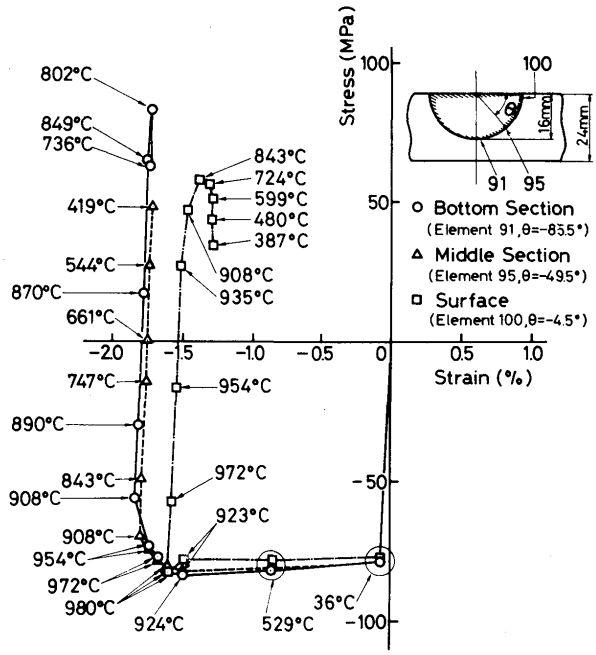

Fig. 12 Stress and Strain behavior in heat affected zone adjacent to fusion line (Conventional Weld Model)

4. Conclusion

Conclusions obtained through the analysis of the temperature and stress distribution during electron beam welding can be summarized as follows:

1) In the nailhead neck area of the heat affected zone, the peak temperature to be heated is higher. Furthermore, the time during which the material is exposed to the nil ductility temperature is longer than in other ones. Such characteristics of the temperature distribution are resultant from the local geometry of electron beam welds which may be regarded as one of some characteristics of weld bead by this welding process.
2) In the nailhead neck area of the heat affected zone, the tensile stress acts nearly in parallel with the fusion line when the material is on cooling through the nil ductility temperature range. Although this stress amount is somewhat smaller than that of the middle section of the heat affected zone, this stress decreases rather gradually with the distance from the fusion line. Accordingly, nailhead neck area has the wider tensile stress zone.
3) It can be supposed from the above-mentioned temperature and stress distribution that microcrack tends to occur in the nailhead neck area of the electron beam welds.
4) In the conventional weld model, the peak temperature to be heated is below 1000 °C and clearly lower than that in the electron beam weld model.
5) In the heat affected zone adjacent to the fusion line of the electron beam weld model and conventional one, the free expansion on heating is almost restrained. Meanwhile, the free shrinkage on cooling is not restrained in the conventional weld model so much as in the electron beam weld model.
6) It can be supposed from the viewpoint of above-mentioned peak tempterature to be heated and internal restraint intensity on cooling that microcrack hardly occur in the conventional welds.

References

1) Y. Arata, K. Terai, H. Nagai, S. Shimizu and T. Aota, "Fundamental Studies on Electron Beam Welding of Heat-resistant Superalloys for Nuclear Plants (Report 1)—Effect of Welding Conditions on Some Characteristics of Weld Bead—", Transactions of JWRI, Vol. 5 (1976), No. 2, p. 119–126.
2) Y. Arata, K. Terai, H. Nagai, S. Shimizu and T. Aota, "Fudamentale Studien zum Elektronenstrahlschweissen von Hitzebestaendigen Legierungen fuer Kernkraftanlagen (Bericht 3)—Metallurgische Betrachtungen ueber Mikroriss—", Transactions of JWRI, Vol. 6 (1977), No. 2, p. 75–90.
3) O.C. Zienkievicz and Y.K. Cheung, "The Finite Element Method in Structural and Continuum Mechanics", MacGraw-Hill, 1967.

4) Y. Yamada, "Plasticity and Viscoelasticity (in Japanese)" Baifukan (1972)
5) Y. Arata, K. Terai, H. Nagai, S. Shimizu and T. Aota, "Fundamental Studies on Electron Beam Welding of Heat-resistant Superalloys for Nuclear Plants (Report 2)—Correlation between Susceptibility to Weld Cracking and Characteristics in Hot Ductility and Trans-Varestraint Test—" Transactions of JWRI, Vol. 6 (1977), No. 1, p. 69–80.